Antitubercular Nanocarrier Combination Therapy: Formulation Strategies and In Vitro Efficacy for Rifampicin and SQ641

Suzanne M. D'Addio[1], Venkata M. Reddy[2], Ying Liu[1], Patrick J.Sinko[3], Leo Einck[2], Robert K. Prud'homme[1]*

[1]*Department of Chemical Engineering, Princeton University, Princeton, NJ 08544*
[2]*Sequella Inc., Rockville, MD 77845*
[3]*Ernest Mario School of Pharmacy, Rutgers University, Piscataway, NJ, 08854*

Supplemental Information

S.1. RIF pro-drug synthesis

Two RIF prodrugs were synthesized by conjugation of RIF to (a) VES or (b) 2 kDa polycapralactone (PCL) (Scheme 1). The conjugation reactions were run at the same conditions, where DMAP (9.2 mg, 0.075 mmol), RIF (124-930 mg, 0.15-1.13 mmol) and DCC (156 mg, 0.754 mmol) were added to a solution of either VES or PCL (0.75 mmol) in DCM (20 ml) at 0 °C. The solutions were protected from light, sparged with nitrogen for 30 minutes, stirred for 5 minutes at 0 °C, and then left to reach room temperature. The reaction proceeded with continuous stirring for 16 h at room temperature. The reaction mixtures were filtered to remove precipitated urea, washed twice with 0.1 N HCl, and dried with $MgSO_4$. The solvent was removed by rotary evaporation.

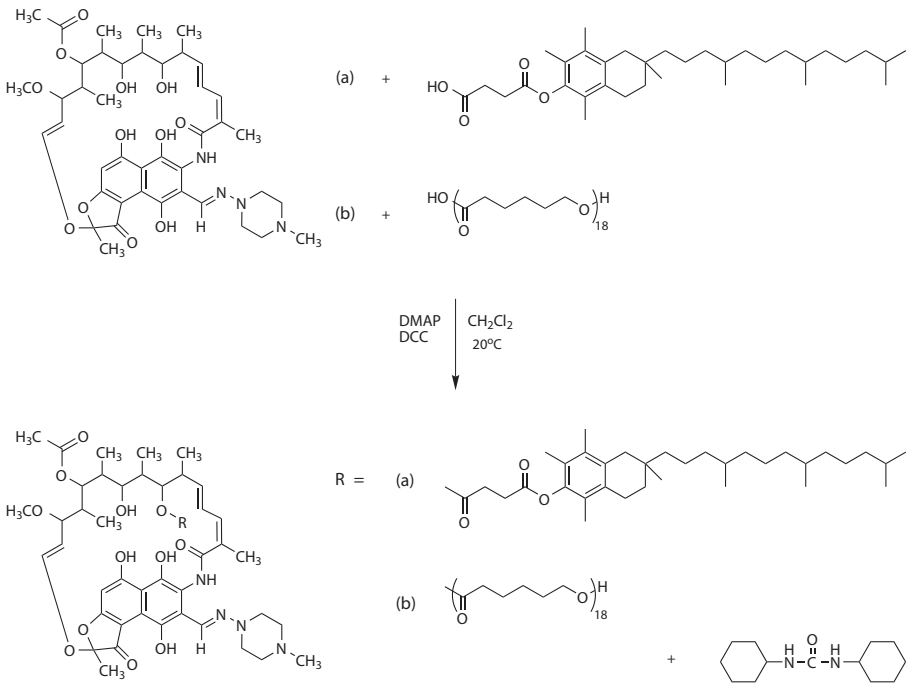

Scheme 1. Synthesis route for the conjugation of Rif via DCC coupling to (a) VE or (b) PCL.

Due to the complexity of ^{1}H NMR peaks of the prodrug, including peak overlap of RIF and VES [1, 2], HPLC was used to quantitatively identify the drug (RIF), the prodrug (RIF-VE or RIF-PCL), and the hydrophobic anchor (VE). PCL is not UV active and therefore could not be detected. A gradient mobile phase was used for separation of the mixture components, allowing for peak resolution (Fig. S1).

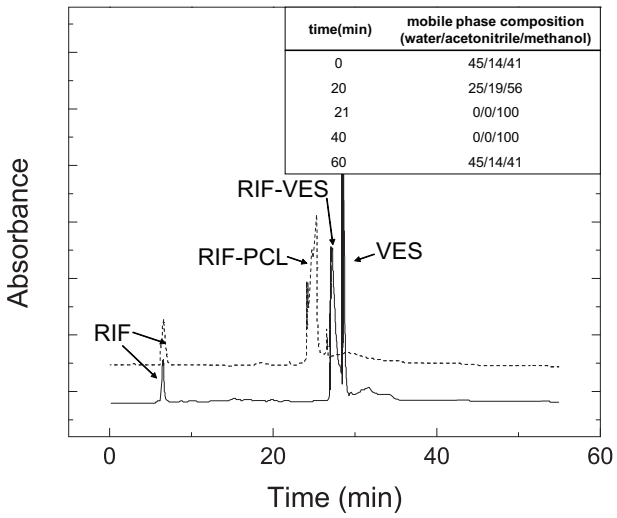

Figure S1. Example chromatograms of prodrug reaction mixtures. Quantification of mixtures of (—) RIF at 6 min, RIF-VE at 27.5 min and VES at 29 min or (---) RIF at 7 min and RIF-PCL at 26 min was achieved by HPLC using a methanol/acetonitrile/water gradient mobile phase (inset) and detection at 284 nm.

HPLC analysis was performed utilizing either (1) a P4000 pump, AS3000 autosampler, and UV2000 detector or (b) a Finnigan Surveryor® PDA Plus Detector, Autosampler Plus autosampler, and LC Pump Plus pump (both Thermo Separation Products. Thermo Electron Corporation, Massachusetts, USA), and separation was achieved with a polar embedded C18 column (Synergi Fusion, 4 µm, 4.6 mm x 150 mm, Phenomenex, Torrance, CA), affording moderate retention of hydrophobic compounds with a detection wavelength of 284 nm. The sample injection volume was 10 µL.

Rifampicin has five hydroxyl groups on the molecule. However, it was confirmed by LS/MS analysis that for Rif-VitE and Rif-PCL, only one site was reacted. An example chromatograph is shown in Fig. S2.

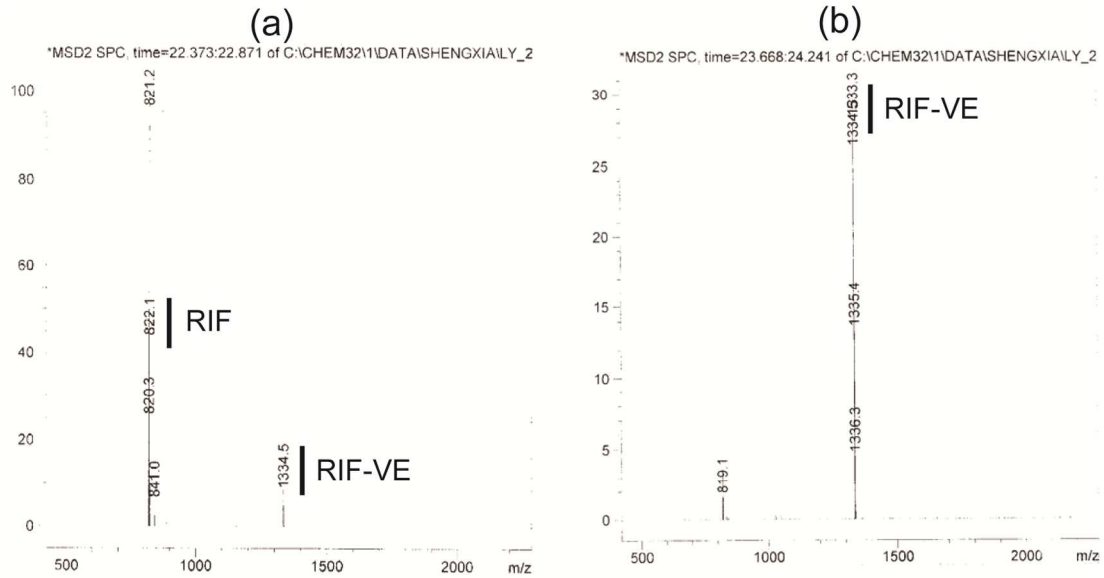

Figure S2. Chromatogram for rifampicin (Mw=822.1) and rifampicin VitE monoconjugate (Mw=1334.5) by LS/MS (a) at 22.4 minutes, and (b) at 23.7 minutes.

S.2. SMILES and calculation of RIF prodrug logP values

(1) RIF-VE

- SMILES:CO[C@H]3C=CO[C@@]7(C)Oc6c(C)c(O)c5c(O)c(NC(=O)C(C)=CC=C[C@H](C)[C@H](OC(=O)CC(=O)Oc2c(C)c(C)c1CC(C)(CCCC(C)CCCC(C)CCC(C)C)CCc1c2C)[C@@H](C)[C@H](O)[C@H](C)[C@H](OC(C)=O)[C@@H]3C)c(C=NN4CCN(C)CC4)c(O)c5c6C7=O
- miLogP 9.654
- MW 1319.729
- Volume 1282.295

(2) RIF-PCL

- SMILES:CO[C@H]1C=CO[C@@]5(C)Oc4c(C)c(O)c3c(O)c(NC(=O)C(C)=CC=C[C@H](C)[C@H](OC(=O)OCCCCOC(=O)CCCCCOC(=O)CCCCCOC(=O)CCCCCOC(=O)CCCCCOC(=O)CCCCCOC(=O)CCCCCOC(=O)CCCCCOC(=O)CCCCCOC(=O)CCCCCOC(=O)CCCCCOC(=O)CCCCCOC(=O)CCCCCOC(=O)CCCCCOC(=O)CCCCCOC(=O)CCCCCO)[C@@H](C)[C@H](O)[C@H](C)[C@H](OC(C)=O)[C@@H]1C)c(C=NN2CCN(C)CC2)c(O)c3c4C5=O
- miLogP 10.616
- MW 2765.373
- Volume 2651.707

(3) RIF

- SMILES:CO[C@H]1C=CO[C@@]5(C)Oc4c(C)c(O)c3c(O)c(NC(=O)C(C)=CC=C[C@H](C)[C@H](O)[C@@H](C)[C@H](O)[C@H](C)[C@H](OC(C)=O)[C@@H]1C)c(C=NN2CCN(C)CC2)c(O)c3c4C5=O
- miLogP 2.615
- MW 822.953
- Volume 755.912

S.3. Redispersion of RIF prodrug nanocarrier formulations

In order to transport and test the efficacy of these nanocarriers against *M. tuberculosis,* a dried form of the formulation was prepared. Previously, Kumar *et al*. used a combination of trehalose and Pluronic F68 as a cryoprotectant during freeze drying to prevent irreversible nanocarrier aggregation [3]. In this work, the same cryoprotectants also protected the nanocarriers against extensive aggregation during freezing and lyophilization. After rehydrating and resuspending the nanocarriers at a concentration of 1 mg mL^{-1} RIF with a moderate period of sonication, all formulations redispersed to less than 500 μm (Fig. S3), which was suitable for dosing and *in vitro* analysis.

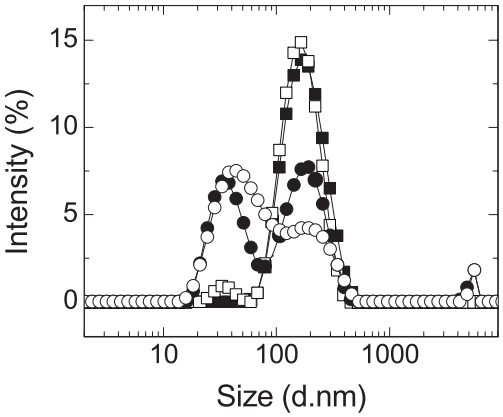

Figure S3. Particle size distribution for RIF The RIF-PCL (NC1, ■) and RIF-VE nanocarriers with RIF core loadings of 0% (NC2, □) to 10% (NC3, ●) and 50% (NC4, ○) after freeze drying with trehalose and Poloxamer® F68 as cryoprotectants. After rehydration, the powders were resuspended by brief hand shaking and probe tip sonication.

The RIF-PCL particles redisperse to 190 nm. The effectiveness of resuspension can be captured in the ratio of the redispersed size, S_f, to the initial size, S_i, where values close to 1 correspond to good resuspension and values much larger than 1 indicate extensive aggregation. For RIF-PCL, S_f/S_i = 1.1, which indicates complete protection from aggregation, within experimental error. In contrast, the RIF-VE particles aggregate, with S_f/S_i = 2.8; however, the final average particle size is 170 nm, which is suitable for injection. There is a smaller population which is present, which corresponds to the primary particle size, prior to lyophilizaiton. Since the intensity weighted particle distribution weights by the sixth power of the size, the number of larger particles is smaller that is represented by the distribution reported by DLS in Fig. S3. As the weight fraction of RIF in the core of RIF-VE formulations increases, the resuspension is better. Two populations are measured by DLS, where the smaller peak corresponds to the primary particle size and the larger peak has an average value that corresponds to a S_f/S_i = 3.4 and 54% of the intensity weighted distribution and S_f/S_i = 6 and 30% of the intensity weighted distribution for NC3 and NC4, respectively. While we present the particle size distribution computed from the correlation function

for the light scattering of the suspensions without transformation of the data, the population of aggregates scatter more light than the smaller populations, and the intensity weighted particle size distributions scales the number of particles to the 6/5 power of the diameter [4]. Therefore, the number population of aggregates is smaller than estimated by dynamic light scattering.

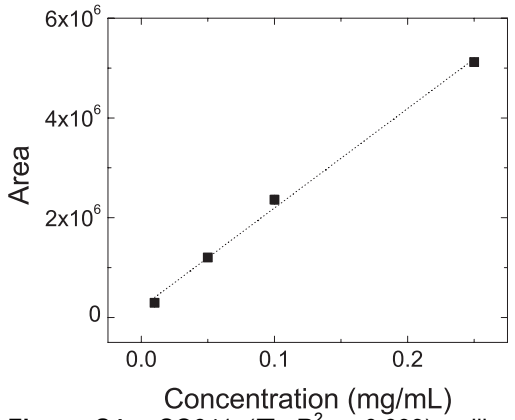

Figure S4. SQ641 (■, R^2 = 0.993) calibration curve for the determination of SQ641 solubility in THF/water mixtures.

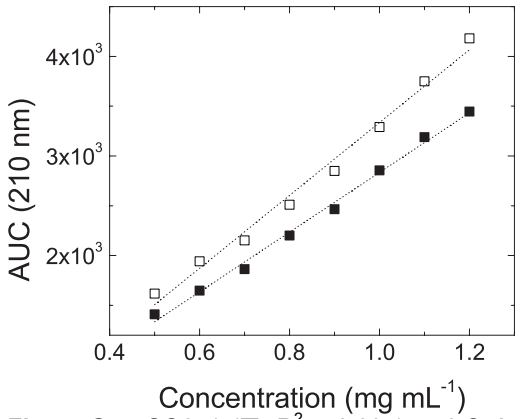

Figure S5. SQ641 (■, R^2 = 0.995) and CsA (□, R^2 = 0.989) calibration curves for analysis of drug concentrations prior to *in vitro* testing.

S.4. Calibration curves

The concentration of SQ641 in standard dilutions was correlated to the integrated area under the curve from the HPLC chromatogram (Fig. S4). Measurements were performed using a Finnigan Surveryor® PDA Plus Detector, Autosampler Plus autosampler, and LC Pump Plus pump (Thermo Electron Corporation, Massachusetts, USA), and separation was achieved with a polar embedded C18 column (Synergi Fusion, 4 µm, 4.6 mm x 150 mm, Phenomenex, Torrance, CA). An isocratic method with a 95% methanol/5% water mobile phase at 1.5 mL min^{-1}, an injection volume of 20 µL, and a detection wavelength of 210 nm was used.

HPLC analysis of dissolved nanocarrier samples was performed with an 80% Methanol/20% Water mobile phase at a flow rate of 1 mL min^{-1}, at ambient temperature in a ZORBAX Eclipse Plus C18 4.6 x 150 mm, 3.5 µm Column with UV detection at 210 nm. Calibration curves for CsA and SQ641 were used to determined the concentration of the drugs in each preparation (Fig. S5).

S.5. SQ641 Nanocarrier suspension stability

The stability of the filtered nanocarrier suspension was tracked by DLS measurements over the 10 days following Flash NanoPrecipitation. After dialysis and filtration as described in the main text, the particles formed with a ratio of 0.5:1 and 1:1 are very stable, as shown by the constant size measured by DLS in Fig. S6. There is more intra- and inter-day variability for the particles formed with 1.5:1 and 2:1

ratios of VE to SQ641. Both of these formulations undergo a slight increase in size over the 10 day period of observation. The cause for the large variability on the first day of measurements is due to shifting of the average value reported for multiple measurements, which does not occur on subsequent days. Each data point and error bar is the average and standard deviation, respectively, of two separate measurements, consisting of at least 10-14 measurements of 10 s each.

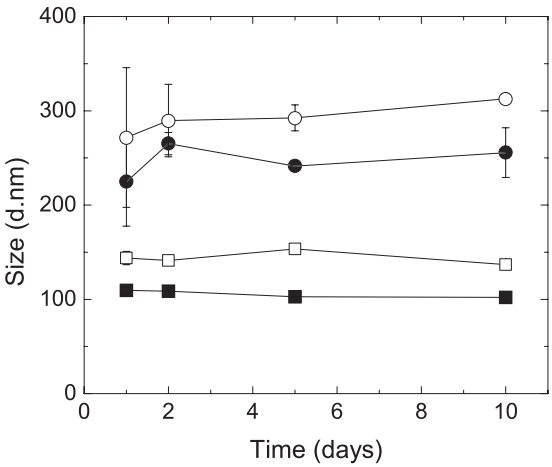

Figure S6. Stability of SQ641 nanocarrier formulations, with VE to SQ641 ratios of 0.5:1 (■), 1:1 (□), 1.5:1 (●), and 2:1 (○). The nanocarrier suspension size is tracked by DLS measurements and the intensity average particle diameter is reported for two replicate measurements, each measurement was the average of 10-14 10 s segments of data collection.

S.6. *In vitro* testing conditions

One of the primary benefits of formulating hydrophobic drugs into block copolymer stabilized nanocarriers is that high concentrations of drug in suspension can be achieved, facilitating the preclinical and clinical testing of drugs at relevant concentrations in aqueous media. In circulation, protected nanocarriers alter the pharmacokinetics of the free drug by extending circulation time and changing biodistribution. Ideally, nanocarrier formulations should be characterized *in vitro*, to determine if the necessary performance criteria, like drug release rates and efficacy, have been met. However, it is not straightforward to develop a discriminating *in vitro* assay for nanocarrier activity against an intracellular pathogen by using cell culture. Nanocarriers are developed to aid in drug delivery in circulation, in which there are flow conditions, the presence of a large volume of hydrophobic “sinks”, and passage through various types of “filtration” organs, like the liver, spleen, and kidney. While “lab on a chip” assays are being developed that mimic *in vivo* conditions more closely, this next generation of materials are only at the prototype stage. As such, incubation of nanocarrier formulations in wells with cells serves as the first stage of comparison against the “soluble” drug to evaluate efficacy. When interpreting the results, only relative comparisons between the formulations can be made under the experimental conditions, and absolute conclusions regarding the ability of a formulation to eradicate an infection cannot be made.

To determine the proper conditions so that significant comparisons could be made, J774.A1 mouse macrophages were infected with *M. tuberculosis* (pSMT1) and were incubated with different test formulations in triplicate for 1 d or 4 d at a concentration of 1xMIC or 2xMIC. The results for the formulations tested are compiled in Fig. S7, in terms of the % control for the given experiment.

At 2xMIC, all formulations with anti-TB drugs have significant activity, and it is not possible to discriminate the different activities. Furthermore, a 4 d incubation time is not very realistic for infected cell exposure to drug concentrations from a single dose. At 1xMIC and only a 1 d exposure, there is not appreciable activity for any of the anti-TB formulations tested. Incubating the infected cells with drugs/formulations at 2xMIC for 1 day permitted for activity of the formulations to be determined, while also having insignificant effects on *M. tuberculosis* activity caused by control formulations. Therefore, this condition was used for all in vitro efficacy data presented.

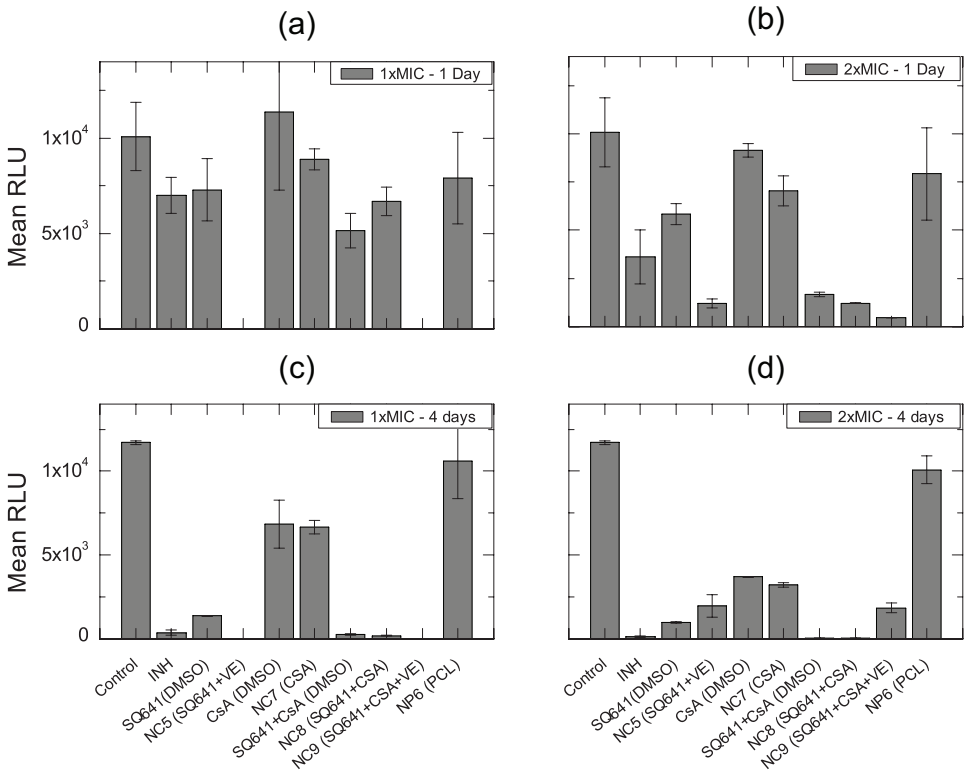

Figure S7. Anti-TB drugs and nanocarrier formulations tested against J774A.1 cells infected with with M. tuberculosis (a) at 1xMIC with an exposure time of 1 d, (b) at 2xMIC with an exposure time of 1 d, (c) at 1xMIC with an exposure time of 4 d, and (d) at 2xMIC with an exposure time of 4 d.

S.7. *In vitro* results significance testing

Table S1. p-values for two tailed Student's t test comparing formulation efficacy against *M. tuberculosis* in Fig. S7.

	Control	INH	SQ641 (DMSO)	NC5 (SQ641+VE)	CsA (DMSO)	NC7 (CSA)	SQ641+CsA (DMSO)	NC8 (SQ641+CSA)	NC9 (SQ641+CSA+VE)
INH	0.028[a]								
SQ641 (DMSO)	0.054[b]	0.096							
NC5 (SQ641+VE)	0.017	0.1	0.008						
CsA (DMSO)	<.8	0.024	0.005	0.031					
NC7 (CSA)	0.2	0.07	0.12	0.008	0.05				
SQ641+CsA (DMSO)	0.019	0.15	0.008	0.098	<.0005	0.009			
NC8 (SQ641+CSA)	0.017	0.099	0.007	>.8	<.0005	0.008	0.011		
NC9 (SQ641+CSA+VE)	0.014	0.065	0.006	0.039	<.0005	0.007	0.004	<.0005	
NC6 (PCL)	0.59	.099	.032	.044	.48	.621	.048	.044	.038

[a] $p \leq 0.05$, gray, significant difference
[b] $p > 0.05$, white, insignificant difference

S.8. References

1. Rubio, E., et al., *NMR spectroscopic analysis of new spiro-piperidylrifamycins.* Magnetic Resonance In Chemistry, 2005. **43**(4): p. 269-282.
2. Baker, J.K. and C.W. Myers, *One-Dimensional And 2-Dimensional H-1-Nuclear And C-13-Nuclear Magnetic-Resonance (Nmr) Analysis Of Vitamin-E Raw-Materials Or Analytical Reference-Standards.* Pharmaceutical Research, 1991. **8**(6): p. 763-770.
3. Kumar, V., et al., *Stabilization of the Nitric Oxide (NO) Prodrugs and Anticancer Leads, PABA/NO and Double JS-K, through Incorporation into PEG-Protected Nanoparticles.* Molecular Pharmaceutics, 2010. **7**(1): p. 291-298.
4. Hanus, L.H. and H.J. Ploehn, *Conversion of intensity-averaged photon correlation spectroscopy measurements to number-averaged particle size distributions. 1. Theoretical development.* Langmuir, 1999. **15**(9): p. 3091-3100.
5. D'Addio, S.M., et al., *Effects of block copolymer properties on nanocarrier protection from in vivo clearance.* J Control Release, 2012. **162**(1): p. 208-217.